# Products of the Gas-Phase Reactions of OH Radicals with $(C_2H_5O)_2P(S)CH_3$ and $(C_2H_5O)_3PS$

**Ernesto C. Tuazon, Sara M. Aschmann, and Roger Atkinson*,†**

*Air Pollution Research Center, University of California, Riverside, California 92521*

*Received: November 4, 2006; In Final Form: December 5, 2006*

Products of the gas-phase reactions of OH radicals with *O,O*-diethyl methylphosphonothioate [$(C_2H_5O)_2P(S)CH_3$, DEMPT] and *O,O,O*-triethyl phosphorothioate [$(C_2H_5O)_3PS$, TEPT] have been investigated at room temperature and atmospheric pressure of air using *in situ* atmospheric pressure ionization mass spectrometry (API-MS) and, for the TEPT reaction, gas chromatography and *in situ* Fourier transform infrared (FT−IR) spectroscopy. Combined with products quantified previously by gas chromatography, the products observed were: from the DEMPT reaction, $(C_2H_5O)_2P(O)CH_3$ (21 ± 4% yield) and $C_2H_5OP(S)(CH_3)OH$ or $C_2H_5OP(O)(CH_3)SH$ (presumed to be $C_2H_5OP(O)(CH_3)SH$ by analogy with the TEPT reaction); and from the TEPT reaction, $(C_2H_5O)_3PO$ (54−62% yield), $SO_2$ (67 ± 10% yield), $CH_3CHO$ (22−40% yield) and, tentatively, $(C_2H_5O)_2P(O)SH$. The FT−IR analyses showed that the formation yields of HCHO, CO, $CO_2$, peroxyacetyl nitrate [$CH_3C(O)OONO_2$], organic nitrates, and acetates from the TEPT reaction were <5%, 3 ± 1%, <7%, <2%, 5 ± 3%, and 3 ± 2%, respectively. Possible reaction mechanisms are discussed.

## Introduction

Alkyl and aryl phosphates [$(RO)_3PO$], phosphonates [$(RO)_2P(O)R$], phosphorothioates [$(RO)_xP(SR)_{3-x}S$], and phosphonothioates [$(RO)_2P(S)R$], where R = alkyl or aryl, are used as plasticizers, flame retardents, fire-resistant fluids and lubricants, and pesticides.[1,2] These compounds and their precursors may be released into the atmosphere where they can undergo transport and chemical transformations.[3] The kinetics of the atmospheric reactions of a number of simple "model" alkyl phosphates, phosphonates, phosphorothioates and phosphonothioates of structure $(RO)_nP(O)(SR)_{3-n}$, $(RO)_nP(S)(SR)_{3-n}$, $(RO)_2P(O)X$, and $(RO)_2P(S)X$ (R = $CH_3$ or $C_2H_5$ and X = H, $CH_3$, $C_2H_5$, or OCH═$CCl_2$) with OH radicals, $NO_3$ radicals, and/or $O_3$ have been studied.[4−14] Reaction with the OH radical is the dominant atmospheric loss process[4−6,9,11,14] for those alkyl phosphates, phosphonates, phosphorothioates, and phosphonothioates for which data are available. The only alkyl phosphorothioates and phosphonothioates containing a P═S bond studied to date are $(CH_3O)_3PS$, $(CH_3O)_2P(S)SCH_3$, $(C_2H_5O)_2P(S)CH_3$, and $(C_2H_5O)_3PS$,[5,14,15] with the formation of the oxon containing a P═O bond from the OH radical-initiated reactions having been investigated[14,15] in addition to the measurement of the rate constants for their reactions with OH radicals, $NO_3$ radicals, and $O_3$.[5,14]

In this work, we have used *in situ* atmospheric pressure ionization tandem mass spectrometry (API-MS) to investigate the products formed from the OH radical-initiated reactions of *O,O*-diethyl methylphosphonothioate [DEMPT, $(C_2H_5O)_2P(S)CH_3$] and *O,O,O*-triethyl phosphorothioate [TEPT, $(C_2H_5O)_3PS$]. Products of the reaction of OH radicals with TEPT were also investigated using *in situ* Fourier transform infrared (FT−IR) spectroscopy and gas chromatography.

* Author to whom correspondence should be addressed. E-mail: ratkins@mail.ucr.edu. Telephone: (951) 827-4191.

† Also at Department of Environmental Sciences and Department of Chemistry, University of California, Riverside.

## Experimental Methods

Experiments utilizing *in situ* atmospheric pressure ionization mass spectrometry were carried out at 296 ± 2 K and 735 Torr total pressure of purified air at ~5% relative humidity in ~7000 L volume Teflon chambers equipped with two parallel banks of blacklamps for irradiation and a Teflon-coated fan to ensure rapid mixing of reactants during their introduction into the chamber. One of the Teflon chambers was interfaced to a PE SCIEX API III MS/MS direct air sampling, atmospheric pressure ionization tandem mass spectrometer (API-MS).[8,9,11] Experiments utilizing *in situ* Fourier transform infrared (FT−IR) spectroscopy were carried out at 298 ± 2 K and 740 Torr total pressure of synthetic air (80% $N_2$ + 20% $O_2$) in a 5870 L Teflon-coated, evacuable chamber equipped with a multiple reflection optical system interfaced to a Mattson Galaxy 5020 FT−IR spectrometer.[8,9,11] Irradiation was provided by a 24 kW xenon arc lamp, with the light being filtered through a 6 mm thick Pyrex pane to remove wavelengths <300 nm. IR spectra were recorded with 32 scans per spectrum (corresponding to a 1.2 min averaging time) at a full-width-at-half-maximum resolution of 0.7 $cm^{-1}$ and a path length of 62.9 m. In all experiments, hydroxyl radicals were generated in the presence of NO by the photolysis of methyl nitrite in air at wavelengths >300 nm.[5,8,9,11]

Products of the reactions of OH radicals with DEMPT and TEPT were investigated using *in situ* API-MS analyses, and products of the TEPT reaction were investigated using *in situ* FT−IR spectroscopic analyses with concurrent analyses by gas chromatography with flame ionization detection (GC−FID) and also with analyses using only GC−FID. For the GC−FID analyses of TEPT, triethyl phosphate [$(C_2H_5O)_3PO$, TEP] and, in certain experiments, $CH_3CHO$, 100 $cm^3$ volume gas samples were collected from the chamber onto Tenax-TA solid adsorbent, with subsequent thermal desorption at ~250 °C onto a 30 m DB-5 megabore column held at 0 °C (or −40 °C when $CH_3CHO$ was also being analyzed) and then temperature-pro-

10.1021/jp067274e CCC: $37.00 
Published on Web 01/18/2007

grammed to 200 °C at 8 °C $min^{-1}$. This GC column program provided separation of TEP from TEPT and of diethyl methylphosphonate [$(C_2H_5O)_2P(O)CH_3$, DEMP] from DEMPT.[14] On the basis of replicate analyses in the chamber in the dark, the analytical uncertainties for the organophosphorus compounds used were typically ≤3%.

**Experiments with API-MS Analyses.** In these experiments, the chamber contents were sampled through a 25 mm diameter × 75 cm length Pyrex tube at ∼20 L $min^{-1}$ directly into the API mass spectrometer source. The operation of the API-MS in the MS (scanning) and MS/MS [with collision activated dissociation (CAD)] modes has been described previously.[9,11,16,17] Use of the MS/MS mode with CAD allows the "product ion" or "precursor ion" spectrum of a given ion peak observed in the MS scanning mode to be obtained.[16] Both positive and negative ion modes were used in this work, with the majority of the data obtained being in the negative ion mode. In the positive ion mode, protonated water hydrates ($H_3O^+(H_2O)_n$) generated by the corona discharge in the chamber diluent air were responsible for the protonation of analytes. Ions are drawn by an electric potential from the ion source through the sampling orifice into the mass-analyzing first quadrupole or third quadrupole. Neutral molecules and particles are prevented from entering the orifice by a flow of high-purity nitrogen ("curtain gas"), and as a result of the declustering action of the curtain gas on the hydrated ions, the ions that are mass analyzed are mainly protonated molecular ions ($[M + H]^+$) and their protonated homo- and hetero-dimers.[16]

In the negative ion mode, negative ions are generated by the negative corona around the discharge needle. The superoxide ion ($O_2^-$), its hydrates, and $O_2$ clusters are the major negative ions in the chamber diluent air. Other reagent ions, for example, $NO_2^-$ and $NO_3^-$, are then formed from reactions between the primary reagent ions and neutral molecules such as $NO_2$, and instrument tuning and operation were designed to induce cluster formation.[17] The initial concentrations of $CH_3ONO$ and NO, and of DEMPT or TEPT, were ∼$2.4 \times 10^{13}$ molecules $cm^{-3}$ each, and irradiations were carried out for 1.0 min (DEMPT) or 0.5−10 min (TEPT), resulting in 25% reaction of the initially present TEPT after 4.0 min of irradiation (as measured by GC−FID).

**Experiments with FT—IR Analyses.** Irradiations of $CH_3ONO$−NO−TEPT mixtures in dry synthetic air (80% $N_2$ + 20% $O_2$) were carried out in the 5870 L evacuable chamber, and both FT−IR and GC−FID analyses were employed. To coordinate FT−IR and GC analyses, the irradiations were carried out intermittently, each with 5−9 min duration, for up to a total irradiation time of 21 min, with GC−FID analyses during the intervening dark periods and FT−IR spectra of the reaction mixture being recorded before and after each irradiation period. The initial concentrations (in units of $10^{13}$ molecules $cm^{-3}$) employed were as follows: TEPT, 9.74−12.3; $CH_3ONO$, 24.6 (or $(CH_3)_2CHONO$, 19.7); NO, 24.6. A weighed amount of liquid TEPT in a sample tube was introduced into the chamber by heating and flushing with a stream of heated $N_2$ gas. Partial pressures of $CH_3ONO$ (or $(CH_3)_2CHONO$) and NO in calibrated 2-L Pyrex bulbs were measured in a vacuum manifold with a 100 Torr MKS Baratron and flushed into the chamber with $N_2$. An IR calibration of $SO_2$ was obtained by introducing known partial pressures of $SO_2$ into the chamber and recording the IR absorption spectrum.

**Experiments to Measure Formation of TEP and $CH_3CHO$ from TEPT by GC—FID.** Additional irradiations of $CH_3ONO$−NO−TEPT−air mixtures were carried out in a ∼7000 L Teflon chamber, with analysis of TEPT, TEP, and $CH_3CHO$ by GC−FID. The initial reactant concentrations (molecules $cm^{-3}$) were as follows: $CH_3ONO$, ∼$2.4 \times 10^{14}$; NO, ∼$1.2 \times 10^{14}$; TEPT, $(2.24-2.37) \times 10^{13}$. Irradiations were carried out for 2−14 min at 20% of the maximum light intensity. The percentage $O_2$ in the $O_2 + N_2$ diluent was varied, and in these experiments the $O_2$ contents were ∼3%, 21% (air), and ∼85%.

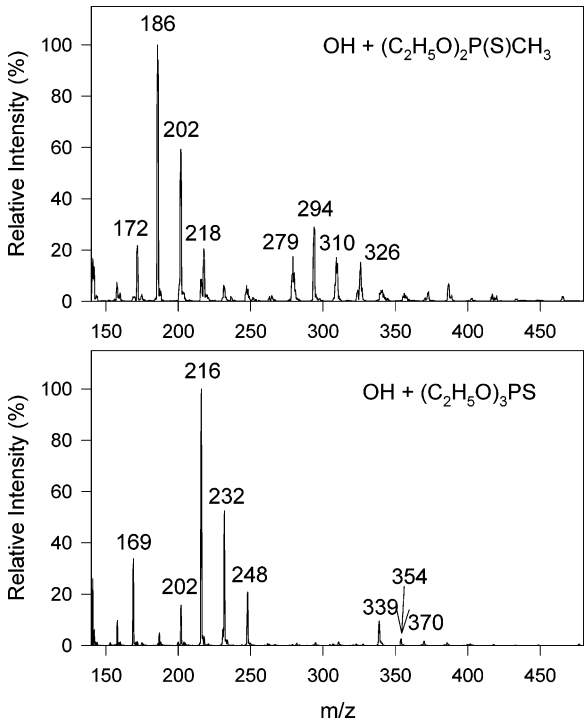


**Figure 1.** Negative ion API-MS spectra of irradiated $CH_3ONO$−NO−DEMPT−air and $CH_3ONO$−NO−TEPT−air mixtures after 1 (DEMPT) or 1.5 min (TEPT) irradiation and after addition of $2.4 \times 10^{13}$ molecules $cm^{-3}$ of $NO_2$. See text for ion peak assignments.

**Chemicals.** The chemicals used, and their stated purities, were as follows: acetaldehyde (99.5%+), diethyl methylphosphonate (97%), *O*,*O*-diethyl methylphosphonothioate (97%), *O*,*O*-diethyl phosphorothioate (potassium salt), and triethyl phosphate (99+%), Aldrich Chemical Co.; *O*,*O*,*O*-triethyl phosphorothioate, Chem Service; NO (≥99.0%) and $SO_2$ (99.98%), Matheson Gas Products. Methyl nitrite was prepared and stored as described previously.[8,9,11]

## Results

**Products of the Reaction of OH Radicals with DEMPT and TEPT by API-MS Analyses.** Irradiations of $CH_3ONO$−NO−DEMPT−air and $CH_3ONO$−NO−TEPT−air mixtures were carried out in a ∼7000 L Teflon chamber at ∼5% relative humidity with analyses by *in situ* API-MS. In the positive ion mode, API-MS spectra of these mixtures prior to irradiation showed the protonated organophosphorus compound monomer at 169 (DEMPT) and 199 (TEPT) and, for the TEPT reaction, the dimer at 397 u. Weak monomer and homo- and heterodimers of DEMP (in the DEMPT reaction) and TEP (in the TEPT reactions) were also observed. No additional ion peaks due to reaction products were observed after irradiation.

In the negative ion mode, no ion peaks attributed to DEMPT or TEPT were observed prior to irradiation. Negative ion API-MS spectra of irradiated $CH_3ONO$−NO−air mixtures of DEMPT and TEPT after 1 min (DEMPT) or 1.5 min (TEPT) irradiation and after addition of $2.4 \times 10^{13}$ molecules $cm^{-3}$ of $NO_2$ are shown in Figure 1. The addition of $NO_2$ to the chamber

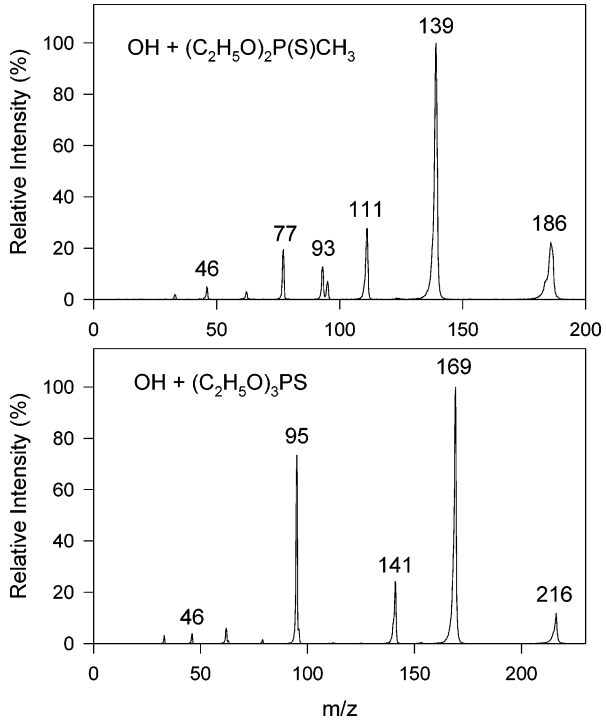


**Figure 2.** Negative ion API-MS/MS "product ion" spectra of the 186 u (DEMPT reaction) and 216 u (TEPT reaction) ion peaks present in the API-MS spectra shown in Figure 1.

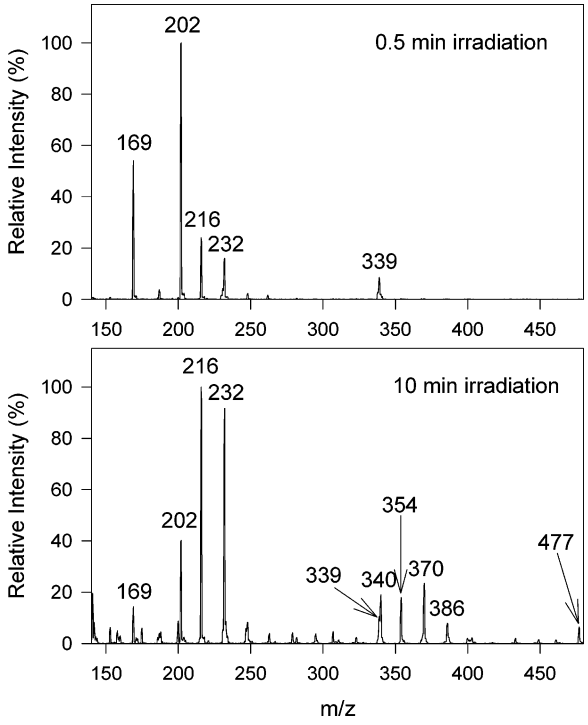


**Figure 3.** Negative ion API-MS spectra of a $CH_3ONO-NO-TEPT-$air mixture after 0.5 and 10.0 min irradiation.

changed the relative intensity of certain of these ion peaks (for example, those at 172 and 186 u in the DEMPT reaction and those at 202 and 216 u in the TEPT reaction) because of differing relative concentrations of $O_2^-$, $NO_2^-$ and $NO_3^-$ reagent ions. API-MS/MS "product ion" and "precursor ion" spectra of the ion peaks shown in Figure 1 were obtained and, as an example, API-MS/MS "product ion" spectra of the 186 and 216 u ion peaks observed in the API-MS spectra of the DEMPT and TEPT reactions, respectively, are shown in Figure 2. The API-MS/MS spectra shown in Figure 2 indicate that the 186 and 216 u ion peaks from the DEMPT and TEPT reactions are $NO_2^-$ adducts of molecular weight 140 and 170 products respectively, with losses of $HNO_2$ and $HNO_2 + 28$ mass units in each case (see also below).

From the API-MS and API-MS/MS spectra, the ion peaks in the API-MS spectrum of the DEMPT reaction shown in Figure 1 are assigned as arising from two products of molecular weights 124 and 140, with the molecular weight 124 product being identical to that previously observed from the OH radical-initiated reaction of DEMP and attributed to $C_2H_5OP(O)(CH_3)$-OH (ethyl methylphosphonate).[9] Thus, the assignments of the ion peaks shown in Figure 1 for the DEMPT reaction are: 172 u, $[140 + O_2]^-$; 186 u, $[140 + NO_2]^-$; 202 u, $[140 + NO_3]^-$; 218 u, $[140 + NO_2 + O_2]^-$; 279 u, $[140 + 140 - H]^-$; 294 u, $[124 + 124 + NO_2]^-$; 310 u, $[124 + 124 + NO_3]^-$; 326 u, $[124 + 124 + NO_2 + O_2]^-$. Similarly, the ion peaks observed from the TEPT reaction (Figure 1) are explained as two products of molecular weight 154 and 170, with the 154 molecular weight product being identical to that observed from the OH radical-initiated reaction of TEP and shown to be diethyl phosphate $[(C_2H_5O)_2P(O)OH$; DEP].[9] The assignments of the ion peaks in Figure 1 for this reaction are then as follows: 169 u, $[170 - H]^-$; 202 u, $[170 + O_2]^-$; 216 u, $[170 + NO_2]^-$; 232 u, $[170 + NO_3]^-$; 248 u, $[170 + NO_2 + O_2]^-$; 339 u, $[170 + 170 - H]^-$; 354 u, $[154 + 154 + NO_2]^-$; 370 u, $[154 + 154 + NO_3]^-$.

Hence, consistent with our previous GC−FID and GC-MS data,[14] the API-MS analyses indicate that the reactions of OH radicals with DEMPT and TEPT lead in each case to two sets of products, a molecular weight 140 product and DEMP from DEMPT, with DEMP reacting further to form the molecular weight 124 product $C_2H_5OP(O)(CH_3)OH$, and a molecular weight 170 product and TEP from the TEPT reaction, with TEP reacting further to form diethyl phosphate, $(C_2H_5O)_2P(O)OH$ (molecular weight 154). Figure 3 shows API-MS spectra from the TEPT reaction after 0.5 min of irradiation (top) and after 10 min of irradiation (bottom). Because of the conversion of NO to $NO_2$ by reaction of NO with $HO_2$ and organic peroxy radicals, $NO_2$ concentrations increase with the extent of reaction and result in differing relative intensities of the ion peaks at 202, 216, 232, and 248 u (see above). Additionally, at larger extents of reaction the intensities of the ion peaks at 340 ($[154 + 154 + O_2]^-$), 354, 370, and 386 u ($[154 + 154 + NO_2 + O_2]^-$) increased relative to those associated with the molecular weight 170 product (i.e., ion peaks at 169, 202, 216, 232, and 248 u). This effect is shown in Figure 4, in which the signal intensities of the ion peaks associated with the molecular weight 170 product (those at 202, 216, 232, and 248) and with $(C_2H_5O)_2P(O)OH$ (those at 354, 370, and 386) are plotted against the irradiation time. In this experiment, irradiations were carried out intermittently, with each API-MS analysis after the irradiation period taking ∼4.5 min for a total duration from beginning the collection of the API-MS spectrum after the first irradiation period to beginning the collection of the API-MS spectrum after the last irradiation period of 51 min. Figure 4 indicates that the molecular weight 170 product is a primary (first-generation) product, while diethyl phosphate, $(C_2H_5O)_2P$-(O)OH, is a second-generation product formed from reaction of TEP, the other first-generation product previously identified by GC-MS and quantified by GC−FID.[14]

The molecular weight 170 product formed from the TEPT reaction (see Figure 4) can be removed by loss to the chamber walls and presumably also by reaction with OH radicals. API-

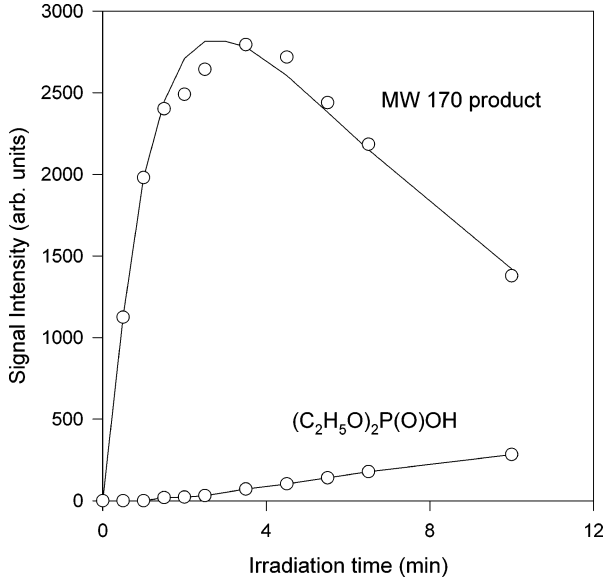


**Figure 4.** Plot of the sum of the signal intensities of the ions at 202, 216, 232, and 248 u assigned to the molecular weight 170 product and of the sum of the signal intensities of the ions at 354, 370, and 386 u due to diethyl phosphate [$(C_2H_5O)_2P(O)OH$] during an irradiation of a $CH_3ONO-NO-TEPT-$air mixture. The solid line for the molecular weight (MW) 170 product is calculated using a reaction rate of TEPT of 0.125 $min^{-1}$, a wall decay rate of the MW 170 product of 0.022 $min^{-1}$, a rate constant ratio of $k$(OH + MW 170 product)/$k$(OH + TEPT) = 4, and assumes that the OH radical concentration was constant (and equal) throughout all the irradiation periods. The line through the $(C_2H_5O)_2P(O)OH$ data is for illustrative purposes only.

MS analyses of a reacted $CH_3ONO-NO-TEPT-$air mixture over a period of 163 min in the dark in a separate experiment with identical initial reactant concentrations suggested a dark loss rate for the molecular weight 170 product of $\sim$0.022 $min^{-1}$. A value of $k$(OH + TEPT)[OH] = 0.125 $min^{-1}$ is derived from the decay of the molecular weight 170 product (Figure 4) over the irradiation time period 4.5−10 min, reasonably consistent with $k$(OH + TEPT)[OH] $\sim$ 0.07 $min^{-1}$ obtained from GC−FID analyses before and after a 4 min irradiation in a separate experiment with similar initial concentrations. The solid line in Figure 4 for the molecular weight 170 product is calculated with $k$(OH + TEPT)[OH] = 0.125 $min^{-1}$, a dark loss rate of the molecular weight 170 product of 0.022 $min^{-1}$, a ratio of $k$(OH + molecular weight 170 product)/$k$(OH + TEPT) = 4, and assuming a constant OH radical concentration during the irradiation periods. Similar fits could be obtained with the molecular weight 170 product undergoing only wall loss at a rate of $\sim$0.1 $min^{-1}$ or only reaction with OH radicals, with $k$(OH + molecular weight 170 product)/$k$(OH + TEPT) $\sim$ 5, or other combinations of wall loss rate and OH radical reaction rate.

The molecular weight 170 product from the OH radical-initiated reaction of TEPT has the formula $C_4H_{11}O_3PS$ and can be attributed to $(C_2H_5O)_2P(S)OH$ or $(C_2H_5O)_2P(O)SH$, with both possible assignments leading to the same ion peaks in the API-MS and API-MS/MS spectra.[18] Thus, both $(C_2H_5O)_2P(S)OH$ and $(C_2H_5O)_2P(O)SH$ have a major ion at 169 u ($[SP(OC_2H_5)_2O]^-$) and fragment ions at 141 u ($[SP(OC_2H_5)(OH)O]^-$) and 95 u ($[SPO_2]^-$),[18] as observed (Figure 2). By analogy with the assignment of the molecular weight 170 product from the OH radical-initiated reaction of TEPT to $(C_2H_5O)_2P(S)OH$ or $(C_2H_5O)_2P(O)SH$, the molecular weight 140 product observed from the DEMPT reaction is attributed to $C_2H_5OP(S)(CH_3)OH$ or $C_2H_5OP(O)(CH_3)SH$. In this case the major ion is at 139 u ($[SP(CH_3)(OC_2H_5)O]^-$) and with a fragment ion at 111 u ($[SP(CH_3)(OH)O]^-$); the fragment ions at 95, 93, and 77 u in Figure 2 may be $[SPO_2]^-$, $[SP(CH_2)O]^-$, and $[SPCH_2]^-$, respectively.

**Products of the Reaction of OH Radicals with TEPT by *in Situ* FT−IR Analyses.** Products of the reaction of OH radicals with TEPT were investigated using *in situ* FT−IR spectroscopy with concurrent GC−FID analyses of TEPT and TEP (see above). The quantitative analysis of products and reactants was carried out by a subtractive procedure,[8,9,11] in which components were successively subtracted from the spectrum of the mixture using calibrated spectra of the gaseous reactants and known products which have been recorded previously with the same instrument and identical spectral parameters. As routinely carried out, the absorption bands of $CH_3ONO$ and NO and of their irradiation products $NO_2$, HCHO, $CH_3ONO_2$, $HNO_3$, and HONO were subtracted first to reveal more clearly the products from the main reactant. $SO_2$ was measured by FT−IR with an estimated accuracy of ±5%. Secondary reaction of the products TEP, HCHO, and $CH_3CHO$ and of the initially present TEP (see below) were taken into account[19] using our previously measured rate constants for the reactions of OH radicals with TEPT[14] and TEP[13] and the IUPAC recommended OH radical reaction rate constants for HCHO and $CH_3CHO$.[20] Corrections for secondary reactions of $SO_2$ were negligible (<1%), and no corrections for secondary reactions were made for other products observed.

In contrast to experiments carried out in our $\sim$7000 L Teflon chamber where the initial concentration of TEP in the chamber after introduction of the $(C_2H_5O)_3PS$ sample was always ≤2.5% (and ≤0.8% for the OH radical reactions),[14] 16−22% of the initially introduced TEPT sample was present as TEP, and $SO_2$ was also initially present at comparable concentrations to TEP, with $([SO_2]/[TEP])_{initial}$ ranging from 0.68 to 1.10. These observations indicate that introduction of TEPT into the evacuable chamber led to significant conversion of TEPT to TEP plus $SO_2$ during the introduction process. Irradiation of $CH_3ONO-NO-TEPT-$air mixtures showed the formation of TEP and $SO_2$, with an $SO_2$ formation yield of 67 ± 10% being obtained from a least-squares analysis of the data and with the indicated error being two least-squares standard deviations combined with uncertainties in the analyses of TEPT and $SO_2$ of ±10% and ±5%, respectively. After correcting for the presence of the initial TEP and for the reaction of TEP with OH radicals, a least-squares analysis resulted in a TEP formation yield of 62 ± 12%, where the indicated error is two-least-squares standard deviations combined with uncertainties in the TEPT and TEP analyses of ±10% each, and with the ranges of the TEP formation yields for the individual experiments being 61−66% and 51−57%. While this TEP formation yield is subject to significant uncertainties because of the presence of initial TEP concentrations which were 53−58% of the final measured TEP concentrations, it is in good agreement with the 56 ± 9% formation yield obtained from experiments conducted in Teflon chambers at 298−299 K with initial TEP concentrations ≤1.2% of the initial TEPT concentrations,[14] and with a 54 ± 12% yield determined in a set of independent experiments carried out in a $\sim$7000 L Teflon chamber at 296 ± 2 K in the present study (see below and Table 1).

**Identity of the Molecular Weight 170 Product: $(C_2H_5O)_2P(S)OH$ or $(C_2H_5O)_2P(O)SH$?** A study of the infrared spectra of *O,O*-diethyl phosphorothioate [$(C_2H_5O)_2P(S)OH$ or $(C_2H_5O)_2P(O)SH$] in the vapor, solution, and condensed phases was carried out to identify the absorption features that could help determine which of the two structural isomers of the molecular weight

**TABLE 1: Products Observed from the OH Radical-initiated Reaction of TEPT and Their Molar Formation Yields**

| | % molar yield[a] | | |
|---|---|---|---|
| product | evacuable chamber[b] | Teflon chamber[c] | ref14[c] |
| $(C_2H_5O)_3PO$ (TEP) | 62 ± 12 | 54 ± 12 | 56 ± 9 |
| $SO_2$ | 67 ± 10 | | |
| $CH_3CHO$ | 22 ± 6[d] | 40 ± 8[d] | |
| HCHO | <5[d] | | |
| CO | 3 ± 1 | | |
| $CO_2$ | <7[d] | | |
| $CH_3C(O)OONO_2$ (PAN) | <2[d] | | |
| $RONO_2$ | 5 ± 3[d] | | |
| $ROC(O)CH_3$ | 3 ± 2[d] | | |
| $(C_2H_5O)_2P(O)SH$ | observed[e] | observed[f] | |

[a] The uncertainties in these formation yields are two standard deviations combined with estimated overall measurement uncertainties in the GC−FID or FT−IR analyses of ±10% for TEPT, ±10% for TEP, ±5% for HCHO, ±10% (GC−FID) or ±20% (FT−IR) for $CH_3CHO$, ±15% for PAN, ±30% for $RONO_2$, ±40% for $ROC(O)CH_3$, ±7% for CO, and ±7% for $CO_2$. [b] Products measured by FT−IR spectroscopy, except for TEPT and TEP which were measured by GC−FID. [c] Measured by GC−FID unless noted otherwise. [d] At ≥21% $O_2$ content in the Teflon chamber (see text). Yields corrected for formation from the OH radical reaction with TEP.[9] The $CH_3CHO$ yields uncorrected for formation from TEP were 26 ± 6% for the evacuable chamber experiments, and 42 ± 8% for the Teflon chamber experiments at ≥21% $O_2$ content. Rate constants used to correct for secondary reactions with OH radicals were taken from Aschmann and Atkinson[14] for TEPT, Aschmann et al.[13] for TEP, and IUPAC[20] for $CH_3CHO$ and HCHO. [e] FT−IR spectral data rule out significant formation of $(C_2H_5O)_2P(S)OH$ and are suggestive of the product being $(C_2H_5O)_2P(O)SH$ (see text). [f] From API-MS analyses (see text), which provide a molecular weight of 170, but no isomer-specific identification.

170 product (i.e., containing the P═O or the P═S group) was formed during the TEPT reaction. The free acid (obtained from the potassium salt by treatment with concentrated HCl, salting out with $NH_4Cl$, and extraction with benzene) is a liquid which was easily introduced into the evacuated chamber with moderate heating and flushing with a flow of heated $N_2$ gas. However, its introduction into the chamber at atmospheric pressure was considerably more difficult, with some polymerization and decomposition occurring upon increased application of heat. The vapor-phase spectra of *O*,*O*-diethyl phosphorothioate obtained with the sample introduced into the evacuable chamber at total pressures of <10 and 740 Torr are shown, respectively, in traces A and B of Figure 5. For comparison, the vapor-phase spectra of diethyl phosphate, TEPT and TEP are also included in Figure 5. The spectra in Figure 5 show similar strong absorptions at around 1050 $cm^{-1}$ for each compound, attributed to the P−O−C groups, along with several similarities in the shapes and positions of the medium and weak bands which greatly complicated the spectral analysis.

Traces A and B of Figure 5 both show a narrow band at 3656 $cm^{-1}$, indicative of a stretching absorption by a nonassociated O−H group in the vapor phase. In addition to forming ethene from sample decomposition/polymerization (estimated as <5% of the sample introduced; ethene absorptions have been subtracted in Figure 5B), introduction of *O*,*O*-diethyl phosphorothioate into the chamber at atmospheric pressure (Figure 5B) resulted in changes in the spectrum relative to that recorded at <10 Torr (Figure 5A). These included a decrease in the intensity of the 3656 $cm^{-1}$ band, the growth of an absorption band at 1282 $cm^{-1}$, and the reversal in intensities of the pair of bands at 970 and 916 $cm^{-1}$. The 1282 $cm^{-1}$ band is most likely the P═O stretch, with its counterparts in TEP and diethyl phosphate

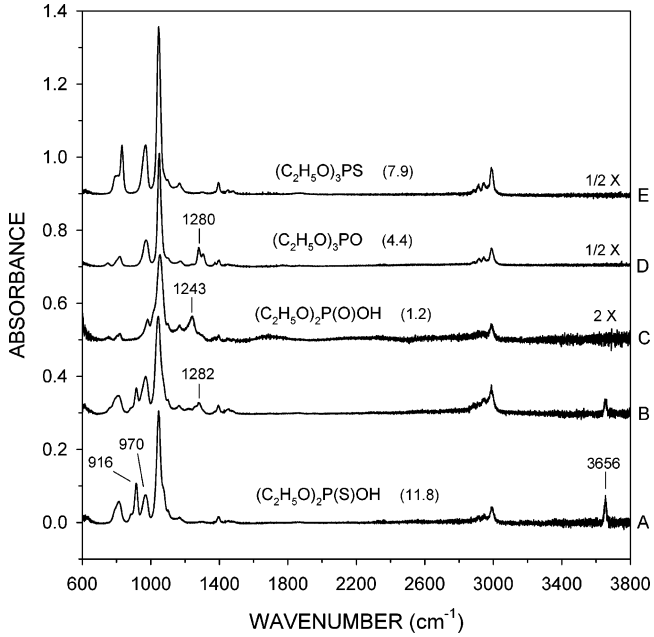


**Figure 5.** Vapor-phase IR spectra: (A) thiono form of *O*,*O*-diethyl phosphorothioate, (B) sample containing both thiono and thiol isomers of *O*,*O*-diethyl phosphorothioate, (C) diethyl phosphate, (D) triethyl phosphate, and (E) *O*,*O*,*O*-triethyl phosphorothioate. Numbers in parentheses are concentrations in units of $10^{13}$ molecules $cm^{-3}$. See text for details.

occurring at 1280 and 1243 $cm^{-1}$, respectively.[9] Comparison of the spectra A and B in Figure 5 at an expanded scale showed that the 1282 $cm^{-1}$ absorption is not present to any measurable extent in Figure 5A, and the latter can be considered to be predominantly the spectrum of the thiono form of *O*,*O*-diethyl phosphorothioate, $(CH_3CH_2O)_2P(S)OH$, with the 3656 and 916 $cm^{-1}$ bands differentiating it uniquely from the spectrum of the thiol form, $(CH_3CH_2O)_2P(O)SH$. Further corroborating information is obtained from a study of solution-phase spectra.

Figure 6 shows spectra of (A) a 0.011 M solution of *O*,*O*-diethyl phosphorothioate in $CCl_4$ solution, (B) the same sample in the cell after 78 min, and (C) a fresh sample of the same solution after standing in a ground-glass stoppered vial for 27 days, with these three spectra being recorded in a 1.01 mm KBr liquid cell and referenced against $CCl_4$ spectra recorded using the same cell. Gaps in the traces represent regions that are interfered with and distorted by the strong absorption bands of the solvent $CCl_4$ and atmospheric $CO_2$. Also presented in Figure 6 is the spectrum of a thin film of an *O*,*O*-diethyl phosphorothioate sample on a KBr plate (D) and the spectrum of the film after a 5-min exposure to a stream of ~2% $O_3$ in $O_2$ (E). All the spectra in Figure 6 were recorded with a deuterium triglycine sulfate (DTGS) detector, which is less sensitive than the mercury cadmium telluride (HgCdTe) detector routinely employed in the present studies but which enabled the lower frequency region down to 400 $cm^{-1}$ to be recorded.

Figure 6A shows absorptions which generally correspond with those of the vapor spectrum of Figure 5A and has bands at 3595 and 915 $cm^{-1}$ whose intensities are greatly diminished after 78 min (Figure 6B), accompanied by the growth of an absorption band at 1262 $cm^{-1}$ in the P═O stretch region. Consistent with the assignment of the 3595 and 915 $cm^{-1}$ bands (3656 and 916 $cm^{-1}$ in the vapor phase) as unique to the thiono form, the spectral changes observed in Figure 6, traces A and B, correspond to a shift with time in the composition of the isomeric mixture in $CCl_4$ solvent from one that is predominantly comprised of the thiono form to one that is predominantly of

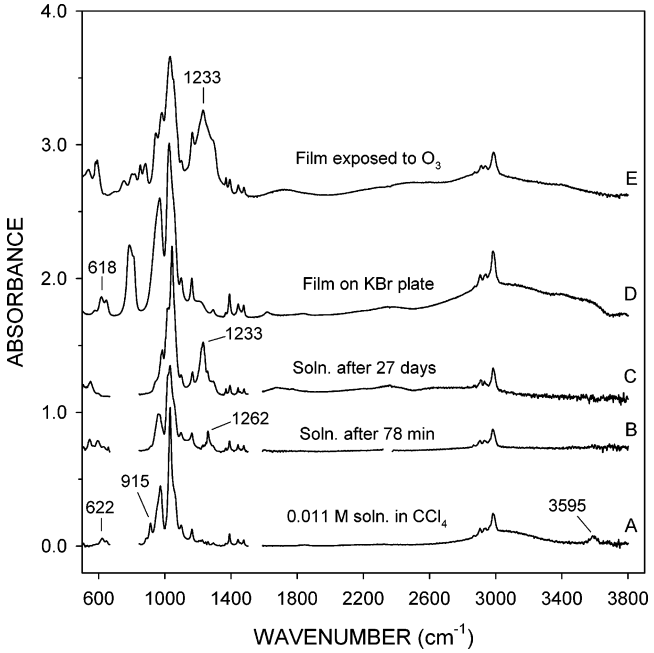


**Figure 6.** IR spectra: (A) *O*,*O*-diethyl phosphorothioate solution in $CCl_4$, (B) same solution sample after 78 min, (C) a fresh sample from the same solution after 27 days, (D) a thin film of *O*,*O*-diethyl phosphorothioate sample on KBr plate, and (E) the same film on KBR plate after exposure to $O_3$. The solution spectra were recorded in a 1.01 mm KBr liquid cell. See text for details.

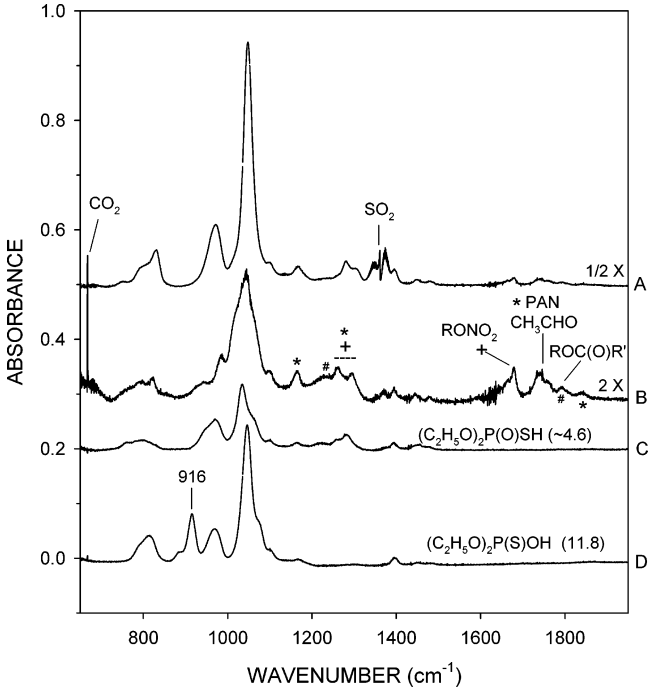


**Figure 7.** IR spectra: (A) *O*,*O*,*O*-triethyl phosphorothioate−$CH_3$-ONO−NO mixture after 21 min of photolysis, with absorption by products of $CH_3ONO$ and NO subtracted, (B) from trace A after subtraction of absorptions by *O*,*O*,*O*-triethyl phosphorothioate, triethyl phosphate, and $SO_2$, (C) thiol form of *O*,*O*-diethyl phosphorothioate, and (D) thiono form of *O*,*O*-diethyl phosphorothioate. Numbers in parentheses are concentrations in units of $10^{13}$ molecules $cm^{-3}$. See text for details.

the thiol form. In Figure 6A, the weak doublet with its maximum at 622 $cm^{-1}$ is in the consensus frequency range ascribed to the P═S stretch.[21,22] After 27 days, the spectrum of the solution of *O*,*O*-diethyl phosphorothioate in $CCl_4$ (Figure 6C) showed the presence of a medium intensity band at 1233 $cm^{-1}$ along with the complete absence of the bands at 3595, 915, and 622 $cm^{-1}$. It should be noted that, although stoppered, the vial containing the $CCl_4$ solution was initially exposed to air. The 1233 $cm^{-1}$ band is consistent with the oxidation of *O*,*O*-diethyl phosphorothioate to diethyl phosphate.

The spectrum of a *O*,*O*-diethyl phosphorothioate film on KBr plate (Figure 6D) shows the weak but distinct peak at 618 $cm^{-1}$ attributed to the P═S stretch, displays the near absence of a P═O stretch, and has good correspondence with Figures 5A and 6A despite the absence of bands near 915 and 3600 $cm^{-1}$. From the foregoing observations, this pair of bands are most certainly associated with the "free" OH group of *O*,*O*-diethyl phosphorothioate, such that the film can still be rationalized as composed primarily of the thiono isomer with the OH groups being involved in intermolecular H-bonding. The broad contours surrounding the C−H stretch region at ∼3000 $cm^{-1}$ are indicative of this molecular association, being observed also in the liquid spectra of other organic phosphates containing the P−OH group.[22,23] The spectrum of the *O*,*O*-diethyl phosphorothioate film exposed to $O_3$ (Figure 6E) showed the disappearance of the P═S band at 618 $cm^{-1}$, and the occurrence of the medium to strong intensity band at 1233 $cm^{-1}$ indicates the formation of diethyl phosphate, which agrees with that observed with the oxidized product in solution (Figure 6C).

The broad contours around the 3000 $cm^{-1}$ region ascribed to molecular association involving the OH group are seen in Figure 6, traces A, D, and E. Indeed, the 0.011 M concentration of *O*,*O*-diethyl phosphorothioate in $CCl_4$ may not be dilute enough to prevent intermolecular association to occur and may largely be the reason for the diminished intensities of the 3595 and 915 $cm^{-1}$ bands (Figure 6A) relative to their counterparts in the vapor-phase spectrum (Figure 5A). In the case of diethyl phosphate, broad bands at ∼1700 and ∼2350 $cm^{-1}$ also occur in solution (Figure 6C) and in the condensed phase (Figure 6E), and a distinct broad feature is present at ∼1700 $cm^{-1}$ in its vapor-phase spectrum (Figure 5C). These features are noted in the literature as being in the spectra of P−OH type compounds in the condensed phase.[22,23] Interestingly, as observed in previous work in this laboratory,[9,11] the vapor-phase spectra of diethyl phosphate and dimethyl phosphate do not show absorptions in the "free" O−H stretch region around 3600 $cm^{-1}$, and the same is true for a solution of diethyl phosphate in a nonpolar solvent such as cyclopentane. These observations suggest that the O−H and the P═O moieties of diethyl phosphate and dimethyl phosphate in the gas phase and in solution are involved in intramolecular hydrogen bonding, an arrangement which does not occur for the O−H and P═S groups of the $(C_2H_5O)_2P(S)$-OH isomer of *O*,*O*-diethyl phosphorothioate.

Figure 7A shows the spectrum from an OH radical-initiated reaction of TEPT (in the 700−1900 $cm^{-1}$ region) corresponding to a total irradiation time of 21 min, from which the absorptions by $CH_3ONO$ and NO and their photo-oxidation products HCHO, $NO_2$, $CH_3ONO_2$, and $HNO_3$, as well as $H_2O$, have been subtracted. The product spectrum shown in Figure 7B resulted from further subtraction of the absorptions of the unreacted TEPT and those of TEP and $SO_2$. The reaction mixture contained $7.9 \times 10^{13}$ molecules $cm^{-3}$ of TEPT at the start of photolysis, with $4.6 \times 10^{13}$ molecules $cm^{-3}$ reacting after 21 min of irradiation.

Apart from being products of the TEPT reaction, both TEP and $SO_2$ were found to be present in the vapor sample of TEPT introduced into the evacuable chamber. Because of the severe overlap of most absorption bands of TEPT and TEP, the quantitative subtraction of their spectra was based on the GC−

FID analyses that were carried out concurrently. The spectra assigned to the two structural isomers of *O,O*-diethyl phosphorothioate are also included in Figure 7 for comparison with the residual spectrum. Figure 7C is a spectrum which is assigned as mostly due to the thiol isomer $(C_2H_5O)_2P(O)SH$, and is derived by subtraction of Figure 5A, the spectrum of the thiono isomer, from Figure 5B based on the cancellation of the 916 $cm^{-1}$ absorption. The spectrum of the thiono isomer $(C_2H_5O)_2P(S)OH$ (Figure 5A) is replotted in Figure 7D. The corresponding concentrations of the thiol (best estimate) and thiono isomers are indicated in Figure 7, traces C and D.

The spectrum of the reaction mixture recorded after each irradiation period did not show a detectable O−H absorption band at or near the 3656 $cm^{-1}$ absorption assigned to the thiono isomer of *O,O*-diethyl phosphorothioate. Moreover, there was a clear absence of the 916 $cm^{-1}$ band, as is evident from a comparison of Figure 7B and Figure 7D. On the basis of the calibrated intensity of the 916 $cm^{-1}$ peak, it was estimated that, if present, $3.5 \times 10^{12}$ molecules $cm^{-3}$ of the thiono isomer would be detectable in the spectrum of Figure 7B. This corresponds to an upper detection limit for the thiono form of <8% of the reacted TEPT.

An overlay of Figure 7C with Figure 7B show coincidences in a number of peaks, but a clear determination on whether the molecular weight 170 product (attributed to *O,O*-diethyl phosphorothioate) detected by API-MS is the thiol form cannot be conclusively made due to interferences from other products, including diethyl phosphate (a product from the OH radical reaction with TEP[9]). Thus, for example, there was no visible change in the contour of Figure 7B upon addition or subtraction of a Figure 7C spectrum that was scaled to a thiol isomer concentration of $\sim 1.2 \times 10^{13}$ molecules $cm^{-3}$ (equal to ~25% of the reacted TEPT).

**Other Reaction Products.** Absorption peaks assigned to PAN [peroxyacetyl nitrate; $CH_3C(O)OONO_2$], $CH_3CHO$, organic nitrates [$RONO_2$], and an ester [$ROC(O)R'$] are indicated in Figure 7B. The PAN and $CH_3CHO$ concentrations were measured by the subtractive procedure using calibrated spectra, with subtraction of the PAN absorptions revealing the underlying band of $CH_3CHO$ at 1745 $cm^{-1}$. The concentration of the organic nitrate(s), $RONO_2$, was estimated from the area of the 1679 $cm^{-1}$ band on the basis of an average absorption coefficient derived from related compounds measured previously in this laboratory.[24] It is possible that there are two $RONO_2$ species involved, since the 1679 $cm^{-1}$ band seen in Figure 7B is broader than is normally observed for an organic nitrate.

The observed ester bands, more clearly seen after subtraction of PAN and $CH_3CHO$ absorptions, are similar to the those of the $RO(CO)CH_3$ product observed from the OH radical-initiated reaction of TEP,[9] and are hence also assigned to an acetate. The acetate concentration was calculated from the 1795 $cm^{-1}$ band, based on an average integrated absorption coefficient of $(1.4 \pm 0.2) \times 10^{-17}$ cm $molecule^{-1}$ derived from the corresponding absorption band areas of ethyl acetate, allyl acetate, and 3-chloropropyl acetate. Note that in our previous product study of the OH radical-initiated reaction of TEP,[9] the average integrated absorption coefficient of $2.3 \times 10^{-17}$ cm $molecule^{-1}$ derived from the characteristic absorption bands of these three acetates at ~1235 $cm^{-1}$ was erroneously reported as the average value for their C=O stretch bands at ~1770 $cm^{-1}$. The acetate formation yield from the TEP reaction is therefore 6% rather than the 4% we previously cited.[9] An additional experiment was carried out to investigate the formation of HCHO and CO, using 2-propyl nitrite as the photolytic precursor to OH radicals. However, this experiment showed that only a very small amount of CO was formed in this reaction, together with only a small amount of HCHO.

We have previously shown that the reaction of OH radicals with TEP in the presence of NO leads to the formation of diethyl phosphate, $(C_2H_5O)_2P(O)OH$, in 65−82% initial yield, together with $CO_2$ (80 ± 10%), HCHO (55 ± 5%), $CH_3CHO$ (11 ± 2%), CO (11 ± 3%), PAN (8%), organic nitrates (7%), and acetates (6%, see above).[9] The amounts of $CO_2$ formed from the secondary reaction of TEP, both initially present and formed from TEPT, accounted for essentially all of the observed $CO_2$, and similarly for HCHO and PAN, noting that PAN formation depends on the $NO_2/NO$ concentration ratio[20] and hence that the PAN formation yield is not expected to be constant throughout a reaction. Assuming that all of the observed HCHO arose from the OH radical-initiated reaction of TEP leads to a HCHO formation yield from the reaction of OH radicals with TEP of 54 ± 18% [from two data points], consistent with our previous directly measured yield of 55 ± 5%.[9] Formation yields, or upper limits thereof, of $CH_3CHO$, HCHO, CO, $CO_2$, PAN, $ROC(O)CH_3$, and $RONO_2$ species from the OH radical-initiated reaction of TEPT, corrected where necessary for secondary formation from TEP, are listed in Table 1. The uncertainties in these formation yields are two standard deviations combined with estimated overall measurement uncertainties in the GC−FID or FT−IR analyses of ±10% for TEPT, ±10% for TEP, ±5% for HCHO, ±10% (GC−FID) or ±20% (FT−IR) for $CH_3CHO$, ±15% for PAN, ±30% for $RONO_2$, ±40% for $ROC(O)CH_3$, ±7% for CO, and ±7% for $CO_2$.

**Formation of TEP and $CH_3CHO$ from TEPT by GC—FID Analysis.** Because of the observed formation of acetaldehyde by FT−IR spectroscopy, additional $CH_3ONO-NO-TEPT-$air irradiations were carried out in a ~7000 L Teflon chamber with analysis of TEPT, TEP, and $CH_3CHO$ by GC−FID. The initial TEP/TEPT concentration ratio was in the range 0.5−1.5%, and the percentage $O_2$ in the $O_2 + N_2$ diluent was ~3%, 21% (air) and ~85%. The $CH_3CHO$ formation yield at the lowest $O_2$ partial pressure (~3% $O_2$) was 0.82 ± 0.13 (two standard deviations) of the average of those measured at 21% $O_2$ and 85% $O_2$. The measured formation yields of $CH_3CHO$ (at ≥21% $O_2$ content) and of TEP are given in Table 1.

If an ethoxy radical is the precursor to $CH_3CHO$, then its reaction with $O_2$

$$C_2H_5O^{\bullet} + O_2 \rightarrow CH_3CHO + HO_2 \qquad (1)$$

is in competition with reactions with NO and $NO_2$ to form ethyl nitrite and ethyl nitrate, respectively.[20]

$$C_2H_5O^{\bullet} + NO\ (+M) \rightarrow C_2H_5ONO\ (+M) \qquad (2)$$

$$C_2H_5O^{\bullet} + NO_2\ (+M) \rightarrow C_2H_5ONO_2\ (+M) \qquad (3)$$

Re-formation of the ethoxy radical plus NO from the photolysis of ethyl nitrite would be only partially effective for the irradiation conditions employed in these experiments (up to 4.5, 6, and 14 min irradiation at $O_2$ contents of ~85%, 21% and ~3%, respectively), since the photolysis lifetime of methyl nitrite in this chamber at this light intensity is ~20 min.[25,26] Using rate constants for reactions 1−3 from the IUPAC evaluation[20] and assuming no re-formation of ethoxy radicals from photolysis of ethyl nitrite, then for the $NO_x$ concentrations used here the $CH_3CHO$ formation yield from the precursor ethoxy radical at 3% $O_2$ content is calculated to be ~65−70% of that at ≥21% $O_2$ content. Given that some re-formation of

**SCHEME 1**

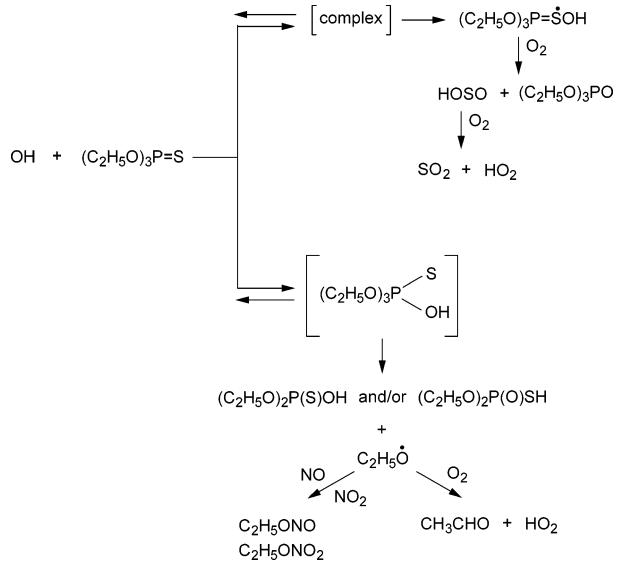


ethoxy radicals from photolysis of ethyl nitrite would have occurred (especially for the longer irradiation times used in the ~3% $O_2$ experiment), the observed slight decrease in $CH_3CHO$ yield at ~3% $O_2$ content compared to that at ≥21% $O_2$ suggests, but does not prove, that ethoxy radicals are formed in the TEPT reaction and are the precursor to $CH_3CHO$. Note that for the analogous reactions of the methoxy radical, in 735 Torr of air in the presence of $2.4 \times 10^{14}$ molecules $cm^{-3}$ of NO + $NO_2$ the overall HCHO yield from the $CH_3O^{\bullet}$ radical is calculated[20] to be ~60−70%. This is consistent with our previous[9] observation of a HCHO yield from the OH radical reaction with TEP of 55 ± 5% compared to that of the expected coproduct $CO_2$ of 80 ± 10%.[9]

Our TEP and $CH_3CHO$ formation yields from experiments carried out in the ~7000 L Teflon chamber, corrected for secondary reactions with OH radicals and for the small amounts of TEP initially present, are given in Table 1 together with the TEP yield from our earlier experiments in this chamber.[14] The TEP yields obtained for the Teflon chamber are slightly lower than measured in the evacuable chamber (although within the experimental uncertainties). In contrast, the $CH_3CHO$ yield in the Teflon chamber with GC−FID analysis is significantly higher than that measured in the evacuable chamber with FT−IR spectroscopy. However, the sum of the TEP (or $SO_2$) plus $CH_3CHO$ yields are more similar, being 84 ± 14% and 89 ± 12% in the evacuable chamber and 94 ± 15% in the Teflon chamber. While GC−FID has a low detection sensitivity for analysis of acetaldehyde, it is also possible that a heterogeneous wall reaction of TEPT occurred in the evacuable chamber, leading to TEP plus $SO_2$ and thereby increasing the observed TEP yield while concurrently decreasing the $CH_3CHO$ yield.

## Discussion

Our previous kinetic measurements show that DEMPT and TEPT are more reactive toward the OH radical than are DEMP and TEP, by factors of 3.6 and 1.5, respectively,[9,13,14] and that $(CH_3O)_3PS$ and $(CH_3O)_2P(S)SCH_3$ are significantly more reactive than $(CH_3O)_3PO$, $(CH_3O)_2P(O)SCH_3$ or $(CH_3S)_2P(O)OCH_3$.[4,5] This increase in OH radical reaction rate constants in compounds containing a P═S bond compared to the corresponding compounds containing a P═O bond indicates a reaction pathway involving the P═S bond,[5] and this is confirmed by the formation of DEMP from DEMPT (in 21 ± 4% yield, independent of temperature over the range 296−348 K) and TEP from TEPT (in 56 ± 9% yield, independent of temperature over the range 296−348 K) as measured by gas chromatography.[14] The formation yields of TEP and $SO_2$ obtained in this work from the OH radical-initiated reaction of TEPT are consistent with the formation of TEP being accompanied by formation of $SO_2$.

The reaction of OH radicals with TEPT appears to form at least one addition complex, based on the highly negative temperature dependence observed recently.[14] The formation of TEP plus $SO_2$ presumably arise from one reaction pathway, while $CH_3CHO$ plus $(C_2H_5O)_2P(O)SH$ appear to be coproducts of a second reaction channel (see below). If only a single intermediate complex is formed which leads to the two sets of products, the $O_2$-independence of the TEP and $CH_3CHO$ yields shows that either both channels are decompositions or both channels involve $O_2$ in the rate-determining step leading to products. Alternatively, two independent complexes may be formed, one leading to TEP plus $SO_2$ and the other to $CH_3CHO$ plus $(C_2H_5O)_2P(O)SH$. In that case, the OH + TEPT reaction to form TEP and $SO_2$ may be analogous to the OH radical reaction with $CS_2$,[20] initially forming a $(C_2H_5O)_3PSOH$ intermediate which then reacts with $O_2$ to form the HOSO radical, with HOSO reacting with $O_2$ to form $SO_2$.

$$OH + (C_2H_5O)_3PS \rightarrow (C_2H_5O)_3PSOH \quad (4)$$

$$(C_2H_5O)_3PSOH + O_2 \rightarrow (C_2H_5O)_3PO + HOSO \quad (5)$$

$$HOSO + O_2 \rightarrow SO_2 + HO_2 \quad (6)$$

TEP then reacts with OH radicals, with the reaction products being $(C_2H_5O)_2P(O)OH$ plus $CO_2$ + HCHO or PAN as coproducts from a major reaction pathway (80−90%) and with a more minor pathway leading to $CH_3CHO$ production (11 ± 2%).[9]

API-MS analyses of the OH radical-initiated reactions of DEMPT and TEPT indicate that another reaction pathway leads to the formation of a molecular weight 140 product from DEMPT, attributed to $C_2H_5OP(S)(CH_3)OH$ or $C_2H_5OP(O)(CH_3)SH$, and a molecular weight 170 product from TEPT, attributed to $(C_2H_5O)_2P(S)OH$ or $(C_2H_5O)_2P(O)SH$. The *in situ* FT−IR analyses of the OH radical-initiated reaction of TEPT showed that $(C_2H_5O)_2P(S)OH$ was not formed to any significant extent, and suggest that the molecular weight 170 product is $(C_2H_5O)_2P(O)SH$. In our previous studies of the reactions of OH radicals with DEMP and TEP,[9] analogous products were postulated to arise after H atom abstraction from the $CH_2$ portion of the $CH_3CH_2O-$ groups, leading, after $O_2$ addition and reaction of the resulting peroxy radical with NO, to the $(C_2H_5O)_2P(O)OCH(O^{\bullet})CH_3$ alkoxy radical from TEP. Through a rearrangement similar to that observed for alkoxy radicals of structure $RC(O)OCH(O^{\bullet})R'$ formed from esters,[27,28] the observed diethyl phosphate[9] would then be formed

$$(C_2H_5O)_2P(O)OCH(O^{\bullet})CH_3 \rightarrow (C_2H_5O)_2P(O)OH + CH_3C^{\bullet}O \quad (7)$$

with subsequent reactions of the acetyl radical leading to formation of $CH_3C(O)OONO_2$ (PAN) or $CO_2$ plus (in part) HCHO.[9]

While an analogous reaction scheme to that proposed for the OH radical-initiated reactions of TEP and DEMP would indeed result in formation of $(C_2H_5O)_2P(O)SH$, the formation yields of the expected coproducts (PAN, $CO_2$, and HCHO) are very

low (Table 1), and the observed amounts of these products can be accounted for by secondary formation from TEP. However, our observation of $CH_3CHO$ suggests that the reaction channel leading to $CH_3CHO$ and $(C_2H_5O)_2P(O)SH$ is an addition−elimination process

$$OH + (C_2H_5O)_3PS \leftrightarrow [(C_2H_5O)_3P(S)OH] \rightarrow C_2H_5O^{\bullet} + [(C_2H_5O)_2P(S)OH \text{ and/or } (C_2H_5O)_2P(O)SH] \quad (8)$$

with subsequent reactions of the ethoxy radical leading to $CH_3CHO$. The proposed reaction mechanism leading to TEP plus $SO_2$ and to $(C_2H_5O)_2P(S)OH$ and/or $(C_2H_5O)_2P(O)SH$ plus $CH_3CHO$ (and ethyl nitrite and ethyl nitrate at sufficiently high NO and $NO_2$ concentrations) is summarized in Scheme 1.

Alternatively, $CH_3CHO$ could arise after H atom abstraction from one of the $CH_2$ groups, followed by reactions with $O_2$ and then NO to form the alkoxy radical,

$$OH + (C_2H_5O)_3PS \rightarrow H_2O + (C_2H_5O)_2P(S)OC^{\bullet}HCH_3 \quad (9)$$

$$(C_2H_5O)_2P(S)OC^{\bullet}HCH_3 + O_2 \rightarrow (C_2H_5O)_2P(S)OCH(OO^{\bullet})CH_3 \quad (10)$$

$$(C_2H_5O)_2P(S)OCH(OO^{\bullet})CH_3 + NO \rightarrow (C_2H_5O)_2P(S)OCH(O^{\bullet})CH_3 + NO_2 \quad (11)$$

followed by

$$(C_2H_5O)_2P(S)OCH(O^{\bullet})CH_3 \rightarrow CH_3CHO + (C_2H_5O)_2P(S)O^{\bullet} \quad (12)$$

Subsequent (and unknown) reactions of the $(C_2H_5O)_2P(S)O^{\bullet}$ radical would then lead to $(C_2H_5O)_2P(S)OH$ and/or $(C_2H_5O)_2P(O)SH$. In this case, the $CH_3CHO$ yield would not be expected to show a dependence on $O_2$ content between 3% and 85% $O_2$.

Our product data (Table 1) show that for the reaction of OH radicals with TEPT, the pathway leading to formation of TEP plus $SO_2$ accounts for 60 ± 12% and the pathway leading to $CH_3CHO$ plus $(C_2H_5O)_2P(O)SH$ accounts for ∼30 ± 15% of the overall reaction. Our previously reported formation yields for DEMP from the OH radical-initiated reaction of DEMPT (21 ± 4%, independent of temperature over the range 296−348 K) suggests that the reaction pathway leading to DEMP plus $SO_2$ from DEMPT accounts for 21 ± 4% of the overall reaction. The room-temperature partial rate constants for the formation of DEMP (plus $SO_2$) from DEMPT [$(4.2 \pm 1.0) \times 10^{-11}$ cm$^3$ molecule$^{-1}$ s$^{-1}$][14] and of TEP plus $SO_2$ from TEPT [$(4.6 \pm 1.1) \times 10^{-11}$ cm$^3$ molecule$^{-1}$ s$^{-1}$] are essentially identical, suggesting that interaction of the OH radical with the P═S group occurs at the same rate in both DEMPT and TEPT and adding credence to there being two independent pathways, one leading to $SO_2$ plus DEMP or TEP after initial addition of the OH radical to the S atom, and the other leading to $CH_3CHO$ plus $C_2H_5OP(O)(CH_3)SH$ or $(C_2H_5O)_2P(O)SH$ after initial addition of the OH radical to the P atom (reaction 8) or (less likely) after an overall H atom abstraction process (reaction 9).

**Acknowledgment.** The authors thank ENSCO, Inc. for supporting this research. While this research has been funded by this agency, the results and content of this publication do not necessarily reflect the views and opinions of the funding agency. R.A. thanks the University of California Agricultural Experiment Station for partial salary support.

## References and Notes

(1) Toy, A. D.; Walsh, E. N. *Phosphorus Compounds in Everyday Living*; American Chemical Society, Washington, DC, 1987.
(2) *The Pesticide Manual*, 9th ed.; Worthing, C. R., Hance, R. J., Eds.; British Crop Protection Council: Farnham, U.K., 1991.
(3) Atkinson, R.; Arey, J. *Chem. Rev.* **2003**, *103*, 4605.
(4) Tuazon, E. C.; Atkinson, R.; Aschmann, S. M.; Arey, J.; Winer, A. M.; Pitts, J. N., Jr. *Environ. Sci. Technol.* **1986**, *20*, 1043.
(5) Goodman, M. A.; Aschmann, S. M.; Atkinson, R.; Winer, A. M. *Arch. Environ. Contam. Toxicol.* **1988**, *17*, 281.
(6) Atkinson, R.; Aschmann, S. M.; Goodman, M. A.; Winer, A. M. *Int. J. Chem. Kinet.* **1988**, *20*, 273.
(7) Kleindienst, T. E.; Smith, D. F. *Chemical Degradation in the Atmosphere*, Final Report on *The Atmospheric Chemistry of Three Important Volatile Chemical Precursors* to Applied Research Associates, Inc.; U.S. Air Force Contract No. F08635−93.-C-0020; Armstrong Laboratory Environics Directorate: Tyndall AFB, FL, Sept 1996.
(8) Martin, P.; Tuazon, E. C.; Atkinson, R.; Maughan, A. D. *J. Phys. Chem. A* **2002**, *106*, 1542.
(9) Aschmann, S. M.; Tuazon, E. C.; Atkinson, R. *J. Phys. Chem. A* **2005**, *109*, 2282.
(10) Sun, F.; Zhu, T.: Shang, J.; Han, L. *Int. J. Chem. Kinet.* **2005**, *37*, 755.
(11) Aschmann, S. M.; Tuazon, E. C.; Atkinson, R. *J. Phys. Chem. A* **2005**, *109*, 11828.
(12) Feigenbrugel, V.; Le Person, A.; Le Calvé, S.; Mellouki, A.; Muñoz, A.; Wirtz, K. *Environ. Sci. Technol.* **2006**, *40*, 850.
(13) Aschmann, S. M.; Long, W. D.; Atkinson, R. *J. Phys. Chem. A* **2006**, *110*, 7393.
(14) Aschmann, S. M.; Atkinson, R. *J. Phys. Chem. A* **2006**, *110*, 13029.
(15) Atkinson, R.; Aschmann, S. M.; Arey, J.; McElroy, P. A.; Winer, A. M. *Environ. Sci. Technol.* **1989**, *23*, 243.
(16) Aschmann, S. M.; Chew, A. A.; Arey, J.; Atkinson, R. *J. Phys. Chem. A* **1997**, *101*, 8042.
(17) Arey, J.; Aschmann, S. M.; Kwok, E. S. C.; Atkinson, R. *J. Phys. Chem. A* **2001**, *105*, 1020.
(18) Oglobline, A. N.; Elimelakh, H.; Tattam, B.; Geyer, R.; O'Donnell, G. E.; Holder, G. *Analyst* **2001**, *126*, 1037.
(19) Atkinson, R.; Aschmann, S. M.; Carter, W. P. L.; Winer, A. M.; Pitts, Jr., J. N. *J. Phys. Chem.* **1982**, *86*, 4563.
(20) IUPAC, http://www.iupac-kinetic.ch.cam.ac.uk/, 2006.
(21) Gore, R. C. *Discuss. Faraday Soc.* **1950**, *9*, 138.
(22) Pouchert, C. J. *The Aldrich Library of Infrared Spectra*, 2nd ed.; Milwaukee, WI, 1975; pp 483−495.
(23) Pouchert, C. J. *The Aldrich Library of FT-IR Spectra*, 1st ed.; Milwaukee, WI, 1985; Vol. 1, pp 914D-919D and 925D-929D.
(24) Tuazon, E. C.; Atkinson, R. *Int. J. Chem. Kinet.* **1990**, *22*, 1221.
(25) Atkinson, R.; Carter, W. P. L.; Winer, A. M.; Pitts, Jr., J. N. J. *Air Pollut. Control Assoc.* **1981**, *31*, 1090.
(26) Phousongphouang, P. T.; Arey, J. *J. Photochem. Photobiol. A: Chem.* **2003**, *157*, 301.
(27) Tuazon, E. C.; Aschmann, S. M.; Atkinson, R.; Carter, W. P. L. *J. Phys. Chem. A* **1998**, *102*, 2316.
(28) Christensen, L. K.; Ball, J. C.; Wallington, T. J. *J. Phys. Chem. A* **2000**, *104*, 345.